

# Nicotinamide Prevents Retinal Vascular Dropout in a Rat Model of Ocular Hypertension and Supports Ocular Blood Supply in Glaucoma Patients

Simon T. Gustavsson,<sup>1</sup> Tim J. Enz,<sup>2,3</sup> James R. Tribble,<sup>2</sup> Mattias Nilsson,<sup>2</sup> Anna Lindqvist,<sup>1</sup> Christina Lindén,<sup>1</sup> Anna Hagström,<sup>2</sup> Carola Rutigliani,<sup>2</sup> Emma Lardner,<sup>2</sup> Gustav Stålhammar,<sup>2</sup> Pete A. Williams,<sup>2</sup> and Gauti Jóhannesson<sup>1,4,5</sup>

<sup>1</sup>Department of Clinical Sciences, Ophthalmology, Umeå University, Umeå, Sweden

<sup>2</sup>Department of Clinical Neuroscience, Division of Eye and Vision, St. Erik Eye Hospital, Karolinska Institutet, Stockholm, Sweden

<sup>3</sup>Department of Ophthalmology, University of Basel, Basel, Switzerland

<sup>4</sup>Wallenberg Centre for Molecular Medicine, Umeå University, Umeå, Sweden

<sup>5</sup>Department of Ophthalmology, University of Iceland, Iceland

Correspondence: Gauti Jóhannesson, Department of Clinical Sciences, Ophthalmology, Umeå University, Umeå 901 87, Sweden; [gauti.johannesson@umu.se](mailto:gauti.johannesson@umu.se).

Pete A. Williams, Department of Clinical Neuroscience, Division of Eye and Vision, St. Erik Eye Hospital, Karolinska Institutet, Eugeniavägen 12, Solna 171 64, Sweden; [pete.williams@ki.se](mailto:pete.williams@ki.se).

STG and TJE contributed equally to this study as first authors.

PAW and GJ contributed equally to this study as senior authors.

**Received:** June 28, 2023

**Accepted:** October 30, 2023

**Published:** November 27, 2023

Citation: Gustavsson ST, Enz TJ, Tribble JR, et al. Nicotinamide prevents retinal vascular dropout in a rat model of ocular hypertension and supports ocular blood supply in glaucoma patients. *Invest Ophthalmol Vis Sci.* 2023;64(14):34. <https://doi.org/10.1167/iov.64.14.34>

**PURPOSE.** To investigate whether nicotinamide (NAM) modulates retinal vasculature in glaucoma.

**METHODS.** This was a prospective controlled clinical trial investigating animal and human histopathology. Participants included normotensive and ocular hypertensive rats, post-mortem human ocular tissue, glaucoma patients ( $n = 90$ ), and healthy controls ( $n = 30$ ). The study utilized histopathology, computer-assisted retinal vasculature analysis, optical coherence tomography angiography (OCTA), and NAM treatment. The main outcome measures included retinal vascular parameters in rats as assessed by AngioTool; retinal vasculature integrity in rats and humans as assessed by histopathology, antibody-staining, and ImageJ-based measurements; and retinal perfusion density (PD) and flux index in humans as assessed by OCTA.

**RESULTS.** A number of vessel parameters were altered in ocular hypertension/glaucoma compared to healthy controls. NAM treatment improved the retinal vasculature in ocular hypertensive rats, with an increase in mean vessel area, percentage area covered by vessels, total vessel length, total junctions, and junction density as assessed by AngioTool (all  $P < 0.05$ ); vessel wall integrity as assessed by VE-cadherin antibody staining was also improved ( $P < 0.01$ ). In humans, as assessed by OCTA, increases in PD in the optic nerve head and macula complete image (0.7%,  $P = 0.04$  and 1.0%,  $P = 0.002$ , respectively) in healthy controls, and an increase in the temporal quadrant of the macula (0.7%,  $P = 0.02$ ) in glaucoma patients was seen after NAM treatment.

**CONCLUSIONS.** NAM can prevent retinal vascular damage in an animal model of glaucoma. After NAM treatment, glaucoma patients and healthy controls demonstrated a small increase in retinal vessel parameters as assessed by OCTA.

**Keywords:** nicotinamide, retinal vasculature, optical coherence tomography angiography, glaucoma, histopathology

Glaucoma is an irreversible neurodegenerative disease characterized by the progressive dysfunction and loss of retinal ganglion cells (RGCs), whose axons make up the optic nerve and project the electrophysiological signal of the visual circuit to the brain. Glaucoma clinically presents as a deterioration of visual sensitivity, progressive visual field defects, and ultimately irreversible blindness. Affecting ~80 million patients worldwide, with many more undiagnosed, glaucoma is a significant health and economic burden.<sup>1</sup> Age, genetics, and elevated intraocular pressure (IOP) are the major risk factors for glaucomatous neurodegeneration. Current established treatment strategies focus only on IOP

management, a major risk factor that is unlikely to be the sole determinant of the disease. Unfortunately, glaucoma can still progress at an unacceptable rate even when low target pressures are met.<sup>2</sup> More than 40% of patients will progress to monocular blindness during their lifetime despite IOP lowering<sup>3</sup>; thus, a better understanding of the disease and novel, neuroprotective treatment strategies for glaucoma are needed.

Increasing evidence points toward metabolic dysfunction in glaucoma. Retinal ganglion cells are highly metabolically active cells and are sensitive to metabolic perturbations.<sup>4</sup> Metabolic or mitochondrial dysfunction has been identified

at the level of individual cells (retinal ganglion cells in human tissue samples<sup>5</sup> and animal models<sup>6</sup> and other retinal glial cells in animal models<sup>7</sup>) and more generally systemically, as genome-wide association study candidates for genes encoding proteins in metabolic pathways, mitochondrial DNA (mtDNA) mutations, and altered complex I activity in patient lymphoblasts.<sup>8</sup>

Retinal neurons rely on blood-derived glucose for their metabolic needs, as well as metabolite shuttling from neighboring glial cells.<sup>4</sup> Impaired ocular blood flow has been suggested as an additional contributing factor in glaucoma.<sup>9</sup> An increasing body of evidence has demonstrated that vascular compromise is associated with the disease. Studies using optical coherence tomography angiography (OCTA), a relatively new technology that allows quick and non-invasive assessment of the vasculature in the optic nerve head (ONH), peripapillary region, and retina, have shown that there is a good correlation between perfusion parameters and functional and structural parameters such as visual field (VF) indices and optical coherence tomography (OCT) measurements of the ganglion cells and retinal nerve fiber layers.<sup>10</sup> Lower baseline vascular density parameters obtained using OCTA have been shown to be a risk factor for a faster rate of retinal nerve fiber layer (RNFL) decline in glaucoma patients.<sup>11</sup> Furthermore, vascular density parameters, as assessed by OCTA, have been shown to precede functional decline<sup>12,13</sup> and structural decline.<sup>14</sup> In glaucoma suspect eyes, ganglion cell complex (GCC) thickness and macular vessel density were measured over time and showed a decline in vessel density in the absence of a decline in GCC in some cases and, in other cases, a faster vessel density loss than GCC thinning.<sup>15</sup> Thus, agents that aim to protect from vascular dysregulation may be of additional clinical benefit.

Nicotinamide (NAM) is the amide form of vitamin B<sub>3</sub> and a major nicotinamide adenine dinucleotide (NAD) precursor in neurons via the NAD salvage pathway.<sup>16</sup> Mounting evidence has demonstrated that the capacity to maintain NAD pools decreases in many tissues with age, increasing neuronal susceptibility to neurodegenerative diseases such as Alzheimer's disease, Parkinson disease, and glaucoma.<sup>17,18</sup> Bolstering cellular NAD levels to counteract this age- and disease- related change is an attractive therapeutic target. Supporting this, NAM has shown great potential as a novel neuroprotective agent in glaucoma in preclinical studies<sup>6,19–21</sup> and pilot clinical trials.<sup>22,23</sup> In addition to its role in preventing neurodegeneration, directly acting on RGCs, NAM may also have vasoprotective properties through modulation of vasoactive cascades.<sup>24</sup> One potential target, endothelin-1 (ET-1), is a potent vasoconstrictor, and its signaling has been suggested to play a crucial role in vascular dysregulation associated with glaucoma.<sup>25–27</sup> NAM has been shown to counteract ET-1-mediated vasoconstriction on various levels.<sup>28,29</sup> Thus, NAM may protect the ocular vasculature in glaucoma; however, this has yet to be tested.

The aim of the current study was to investigate whether NAM modulates the retinal vasculature in glaucoma. To this purpose, we assessed human ocular tissue from glaucoma patients and animal ocular tissue from a rat model of glaucomatous ocular hypertension (OHT) with or without NAM treatment. To support our findings, we conducted the first in-human study, to the best of our knowledge, using OCTA to directly assess the effect of NAM on the retinal vasculature in patients with different subgroups of glaucoma, includ-

ing primary open-angle glaucoma (POAG), normal-tension glaucoma (NTG), and pseudoexfoliative glaucoma (PEXG), as well as age- and sex-matched healthy controls. POAG, NTG, and PEXG all likely have different pathophysiological mechanisms<sup>30–32</sup> and, therefore, possibly different therapeutic responses to NAM treatment.

## METHODS

### Animal Strain and Husbandry

Animals were housed and fed in a 12-hour light/12-hour dark cycle with food and water available ad libitum. Adult, male Brown Norway rats (12–20 weeks old, weighing 300–400 g; SCANBUR AB, Solna, Sweden) were used in this study. Six rats were used for this study alongside existing tissue from previously published studies, which are described in the following sections. Rats treated with NAM received treated drinking water and a custom diet (to achieve 800 mg/kg/d of NAM as previously described<sup>33</sup>). All breeding and experimental procedures were undertaken in accordance with the ARVO Statement for the Use of Animals in Ophthalmic and Research. Individual study protocols were approved by Stockholm's Committee for Ethical Animal Research (10389-2018).

### Rat OHT Model

Rat OHT was induced using a paramagnetic bead model as previously described.<sup>34</sup> Following 1 week of NAM pretreatment, rats received bilateral injections of microbeads (Dynabeads M-450 Epoxy beads, 4.5- $\mu$ m diameter; Thermo Fisher Scientific, Waltham, MA, USA) prepared in Hank's balanced salt solution (no calcium, no magnesium, no phenol red; Thermo Fisher Scientific). IOP was measured by rebound tonometry (TonoLab; Icare, Vantaa, Finland) prior to OHT induction (day 0) and at 3, 7, 9, 11, and 14 days after OHT induction (rats were awake and unrestrained). IOP recordings were always taken between 9 AM and 10 AM local time to minimize the effects of circadian rhythm on IOP. Rats were euthanized at day 14 by intraperitoneal injection of pentobarbital (75 mg/kg) followed by cervical dislocation. Eyes were immediately enucleated and submerged in 3.7% paraformaldehyde (PFA) in 1 $\times$  phosphate-buffered saline ( $n = 9$ ; OHT-NAM, 800 mg/kg/d).

### Imaging and Analysis of En Face Vascular Morphology in Rat Retina

Blood vessel morphology of the superficial plexus was analyzed from existing images of flatmount rat retinas; eyes were normotensive (NT;  $n = 9$ ), 14-day OHT ( $n = 6$ ), or 14-day OHT-NAM 200 mg/kg/d ( $n = 7$ ), 400 mg/kg/d ( $n = 7$ ), or 800 mg/kg/d ( $n = 10$ ).<sup>33</sup> Retinas were previously stained with isolectin B4 (for marking vascular endothelial cells; Invitrogen *Griffonia simplicifolia* lectin, biotin conjugated, 0.1 mg/mL, #I21414; Thermo Fisher Scientific, Waltham, MA, USA) and visualized with Invitrogen Streptavidin Alexa Fluor 488 Conjugate (4  $\mu$ g/mL, #S11223; Thermo Fisher Scientific). Images had been acquired at the time of staining but not previously analyzed.<sup>33</sup> Vascular imaging and analysis were performed as previously described.<sup>34</sup> The isolectin B4/blood vessel channel was isolated from the image in Fiji, and the background of the image was removed by thresholding. Retinas were cropped to 400,000  $\mu$ m<sup>2</sup>

to maintain consistency (representing >80% of the retinal explant area). AngioTool was used to measure blood vessel morphologies, including area covered by vessels, average vessel thickness, total blood vessel length, total vessel area, average vessel length, total vessel endpoints, total junctions, junction density, and mean lacunarity (a measure of space filling within the image, where a high lacunarity equals less space filling by blood vessels), with the following parameters: blood vessel diameter (8–30  $\mu\text{m}$ ) and pixel intensity (0–255).

### Preparation and Immunofluorescent Labeling of Paraffin-Embedded Rat Eyes

The new OHT–NAM eyes ( $n = 9$ ) were fixed in PFA for 24 hours before paraffin embedding. Eyes were sectioned (sagittal plane) to give ONH sections (3- $\mu\text{m}$  thickness) on a microtome (Microm HM355S Rotary Microtome; Thermo Fisher Scientific). New sections were also cut from existing paraffin embedded control (NT,  $n = 8$ ) and 14-day OHT ( $n = 12$ ) rat eyes, described elsewhere.<sup>34</sup> Sections were first deparaffinized and rehydrated through xylene and an alcohol gradient before performing antigen retrieval using EDTA buffer (pH 9, 20 minutes, 100°C). Antigen retrieval and subsequent labeling were performed using a Bond-III robotic system (Leica Biosystems, Wetzlar, Germany). The sections were then washed and incubated in primary antibody for 60 minutes. Sections were stained with antibody against proteins that are commonly associated with maintaining endothelial junctions and retinal blood barrier integrity; each section was labeled with anti-VE-cadherin (rabbit, IgG, 1:50, #LS-B5971-50; LSBio, Shirley, MA, USA), anti-CD31 (rabbit, IgG, 1:100, #ab182981; Abcam, Cambridge, UK), or anti-claudin-5 (CLDN-5; rabbit, IgG, 1:200, #36-1900; Thermo Fisher Scientific). For visualizing the whole vessel wall and for allowing for differentiation between antibody-stained and non-antibody-stained vessel wall, staining was combined with isolectin B4 (details as above), a marker for vascular endothelial cells. Slides were washed again and incubated in secondary antibody (Invitrogen Goat-anti-Rabbit IgG [H+L] Cross-Adsorbed Secondary Antibody, Alexa Fluor 568, 1:500, #A-11011, and the Streptavidin Alexa Fluor 488 Conjugate, as above) for 15 minutes. Slides were counterstained with 4',6-diamidino-2-phenylindole (DAPI). Sections were dehydrated through an ethanol gradient, cleared in xylene, mounted in Pertex mounting agent (Histolab, Askim, Sweden), and covered with a coverslip.

### Donor Human Eyes Details and Immunofluorescent Labeling

We have previously characterized a cohort of donor human eyes with glaucoma and controls (ocular melanoma without interference on the central retina).<sup>35,36</sup> Access to histopathology archive samples was fully covered through Biobank #366 (St. Erik Eye Hospital, Solna, Sweden). New ONH sections (3- $\mu\text{m}$  thickness;  $n = 6$  glaucoma eyes and  $n = 7$  control eyes) were cut and stained as described above for rat tissue. Anti-CD31 was visualized with a polymer conjugated secondary antibody (BOND Polymer Refine Red Detection; Leica Biosystems). Slides were counterstained with hematoxylin.

### Imaging and Analysis of Internal Vessel Integrity in Rat and Human Retinal Sections

Rat sections were imaged on a Leica DMI8 microscope (Leica Microsystems, Wetzlar, Germany) with a Leica CoolLED pE-300<sup>white</sup> LED-based light source and a Leica DFC7000 T fluorescence color camera. Central vessels at the ONH were imaged and one or multiple peripheral vessels in the nerve fiber layer were imaged on both sides of the retina at  $\sim 1000 \mu\text{m}$  from the ONH. All vessels within the region of interest (ROI) were analyzed, unless the inner lumen was too obscured by residual blood. Human sections were imaged on a ZEISS Axio Scan.Z1 Slide Scanner (ZEISS Microscopy, Oberkochen, Germany). Tiled 40 $\times$  images of the whole ONH and central retina were acquired. The ONH and retina at 2000  $\mu\text{m}$  from the ONH were cropped as ROIs. Vessels were cropped for analysis as above. ImageJ (National Institutes of Health, Bethesda, MD, USA) was used to measure the whole vessel lumen circumference in the selected vessels. The total lengths of all parts of the vessel lumen wall that were positive for VE-cadherin, CD31, or CLDN5 were measured. The ratio of positively stained vessel wall versus total vessel lumen circumference was calculated as a percentage. Mean percentage values were calculated for all central and all peripheral vessels in each eye. Mean values were calculated for each group.

### PROSPECTIVE CLINICAL TRIAL

A prospective clinical trial was conducted at the Eye Clinic at Umeå University Hospital (Umeå, Sweden) between October 2021 and April 2022. The study schedule is presented in Figure 1. Participants in the glaucoma groups ( $n = 90$ ) were recruited from the Eye Clinic at Umeå University

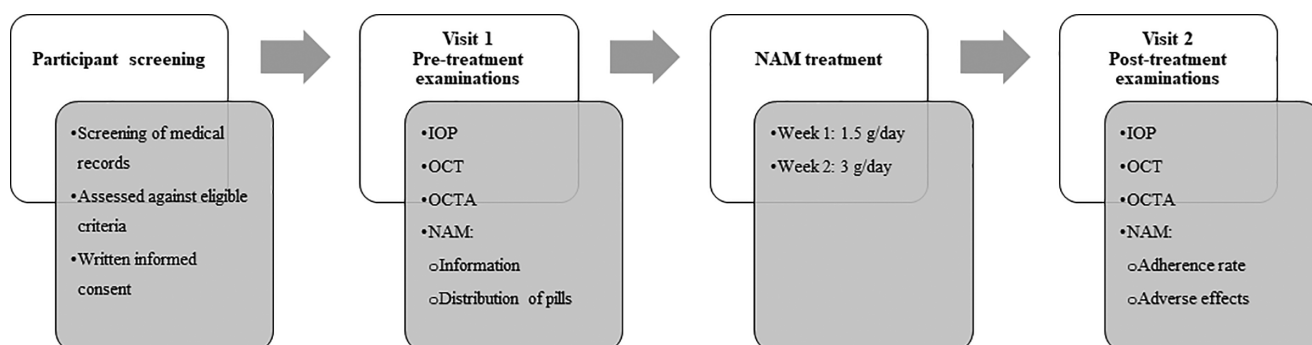


FIGURE 1. Study schedule for the clinical trial. PEX, pseudoexfoliation.



Hospital. Participants in the control group ( $n = 30$ ) were recruited from lists acquired from Statistics Sweden with age- and sex- matched individuals living in the municipality of Umeå. All participants signed a written informed consent prior to entering the study. All testing was performed at the Eye Clinic at Umeå University Hospital.

Inclusion criteria for glaucoma participants included a diagnosis of POAG, NTG, or PEXG in one or both eyes and an age  $>18$  years. Diagnostic criteria for POAG, NTG, and PEXG were based on their respective definitions according to the guidelines of the European Glaucoma Society.<sup>32</sup> Inclusion criteria for age- and sex-matched control participants included being  $>18$  years of age, as well as having a normal VF, a normal optic nerve, and a normal IOP ( $\leq 21$  mmHg) tested at baseline. Study participants performed VF testing within 100 days from the first study visit. In the glaucoma participants, values of the VF mean deviation (MD) were used to grade the severity of glaucoma as “mild” with values higher than  $-6$  decibels (dB), “moderate” with values between  $-6$  and  $-12$  dB, and “severe” with values lower than  $-12$  dB (simplified Hoddaps classification<sup>32</sup>). The VF exam performed in all participants was the standard automated perimetry 24-2 Swedish Interactive Thresholding Algorithm (SITA) of the ZEISS Humphrey Field Analyzer 3 (Carl Zeiss Meditec, Dublin, CA, USA). One eye of each participant was included in the study. Where both eyes in a glaucoma participant were eligible, the eye with the better visual field index (VFI) was chosen. The eye with the better VFI was chosen because it has been shown that vessel density decreases with more severe VF damage,<sup>10</sup> and we expected eyes with a higher vessel density to be more responsive to the possible vascular effects of NAM. A web-based randomization tool was used in the control group to determine which eye of each participant to enroll. Exclusion criteria for both glaucoma and control participants included diseases affecting retinal function (more than mild macular degeneration or diabetic retinopathy), neurological or other non-glaucomatous conditions that may affect the VF, inability to perform a perimetric exam, intake of B vitamins within 1 week before the first study visit and during the study period (aside from NAM within the framework of the study), allergy to NAM/niacin, previous eye surgery involving central parts of the retina, pregnancy/breastfeeding and fertile women not using reliable contraception, diagnosis of cancer in the last 5 years (not including treated squamous cell carcinoma), anamnesis of liver disease or peptic ulcer, and/or not able to speak and understand either Swedish or English.

All of the participants received treatment of NAM (0.5 g NAM tablet; Thorne Research, New York, NY, USA) for 2 weeks. An accelerated dosing strategy was applied to increase tolerability with a dosage of 1.5 g/d (three tablets) the first week and 3.0 g/d (six tablets) the second week. The NAM dosage of 3.0 g/d was based on preclinical<sup>6,33</sup> and clinical<sup>22</sup> trials. For this trial, the same dose was used as in our previous phase II study<sup>22</sup> and is being used in a multicenter phase III clinical trial (NCT05275738). For the animal model work, a known neuroprotective dose was used (800 mg/kg/d,<sup>33</sup> equivalent to 8 g/d for a 60-kg human).<sup>37</sup> The tablets were distributed at the end of the first visit. The treatment started the day after the first visit. Participants were instructed to take 1.5 g in the morning during the first week and 1.5 g twice a day, morning and evening, during the second week. Participants were instructed to take the tablets in conjunction with food to minimize the risk of

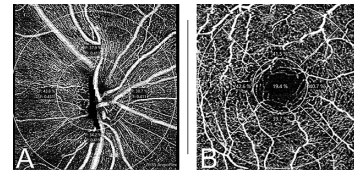


**FIGURE 2.** Example of OCTA scans of the ONH and macula. (A) OCTA scan of the superficial retinal vasculature of the ONH area, with the inner boundary being the inner limiting membrane and the outer boundary being the retinal nerve fiber layer. The perfusion density (P) and flux index (F) are shown for each quadrant. (B) OCTA scan of the macular superficial retinal vasculature, with the inner boundary being the inner limiting membrane and the outer boundary being the inner plexiform layer. The perfusion density is shown for each quadrant and the central region.

gastrointestinal discomfort, which has been reported as the most common side effect in previous clinical trials involving NAM.<sup>22,23</sup> Questions regarding adherence to the treatment and side effects were asked at the second visit. NAM was taken in conjunction with any glaucoma therapies participants were using, and these were factored into the analyses.

Each participant was seen at the first study visit and at posttreatment day 14 ( $\pm 2$  days). At both visits, all participants underwent measurements of IOP and an OCT/OCTA examination. In addition, the healthy controls underwent a slit-lamp examination to determine if pseudoexfoliation material existed on the anterior surface of the lens. Before the examination, pupils were dilated using 0.5% tropicamide (Bausch & Lomb Nordic AB, Stockholm, Sweden). IOP was measured using rebound tonometry (Icare). The exam was repeated if the quality of the measurement was not acceptable. OCT and OCTA scans were performed using the ZEISS CIRRUS 6000, where perfusion density (PD) and flux index analyses were performed using the ZEISS AngioPlex Metrix (Figs. 2A, 2B). PD is defined as the total area of perfused vasculature in the area measured and shown as a percentage. PD is determined by the length and width (inner diameter) of the vessel. Flux index is defined as the total area of perfused vasculature per unit area in the area measured, weighted by the brightness (intensity) of the flow signal. The flux index was only available for ONH analyses. OCT scans were performed of the macular area and ONH area. A macular cube  $512 \times 128$  scan was acquired for the macular area, and the average combined thickness of the ganglion cell layer (GCL) and inner plexiform layer (IPL) was given automatically by the device. For the ONH area, the device acquired an optic disc cube  $200 \times 200$  scan, and the average thickness of RNFL was given automatically.

For the macular area, a  $3 \times 3$ -mm cube-shaped scan, automatically centered on the fovea, was created. The device automatically determined the PD for the superficial vascular plexus, and PD values were given for the following areas: central, inner, and complete. For the inner section, a total PD value was given as well as PD values for each separate quadrant. The inner limiting membrane (inner boundary) and the IPL (outer boundary) defined the superficial vascular plexus. A  $4.5 \times 4.5$ -mm scan was taken for the ONH area, with the ONH area automatically centered in a predefined circle. The PD and flux index was automatically calculated by the device, and values were given for the total area measured, as well as for each separate quadrant. The scan captured the superficial vascular layer, using the inner limiting membrane as the inner boundary and the RNFL as the outer boundary.

Posttreatment scans (macular and ONH) were performed using the manufacturer's "track to prior scan" option, allowing the repeat scan to be tracked and obtained exactly on the baseline scan. Using this option has been shown to increase repeatability.<sup>38</sup> Only OCTA scans with a signal strength of 9 or above were accepted for analyses.<sup>39,40</sup>

In cases where multiple OCTA scans of signal strength 9 or above had been acquired at the first study visit, the highest quality scan was chosen for the study. Where multiple OCTA scans of signal strength 9 or above had been acquired in the posttreatment visit, the first OCTA scan was chosen for the study if deemed of good enough quality for inclusion. If the first scan was not deemed to be of good enough quality, the second scan was chosen and so on. OCTA scans were systematically checked for artifacts, and images with significant motion artifacts or segmentation errors were excluded from the study. In OCTA scans with noticeable segmentation errors and noticeable decentralization of the AngioPlex Metrix overlay, a manual correction was performed in the best way possible. PD and flux index values were hidden throughout the selection process.

The human studies adhered to the tenets of the Declaration of Helsinki, and the ethics protocols were approved by the Swedish Ethical Review Authority (2020-01525, 2021-01036, and 2021-03745). The clinical trial was registered at clinicaltrials.gov (NCT05916066).

Statistical analyses were carried out in SPSS Statistics 28 (IBM, Chicago, IL, USA). All *P* values were two sided and considered statistically significant when they were  $<0.05$ . Normality was tested with the Shapiro-Wilk test. Descriptive statistics were used to describe the study populations' clinical characteristics and are presented as mean and SD, median and interquartile range (IQR), or number and percentage. To check for potential intergroup differences in clinical characteristics, the  $\chi^2$  test was used for categorical variables and ANOVA or the Kruskal-Wallis test was used for scale variables. Post hoc testing was performed when the  $\chi^2$ , ANOVA, or Kruskal-Wallis test was statistically significant. Possible differences in IOP and OCTA parameters after treatment compared to baseline were investigated using a paired *t*-test or Wilcoxon signed-rank test. Pearson's correlation or Spearman's rank correlation was applied to examine correlations among MD (dB), OCTA parameters, and OCT parameters. Multivariate linear regression analyses were performed examining potential factors that influenced the change in IOP and OCTA parameters after NAM treatment. The adherence rate and frequency of side effects were determined using descriptive statistics and are presented as numbers and percentages.

### Nicotinamide Protects From Gross Vascular Morphology Changes in a Rat Model of OHT

Growing evidence suggests that glaucoma is associated with impairment of the retinal vasculature.<sup>9</sup> AngioTool is a publicly available software that was first introduced by Zudaire et al.<sup>41</sup> for the reproducible quantification of vascular networks in microscopic images. The software identifies vascular configuration according to preset parameters, including number of vessels or vessel lengths. For further information on AngioTool and its output values, we refer to the publication of Zudaire et al.<sup>41</sup> To determine how OHT affects the retinal vasculature, we applied AngioTool on retinal explant sections from our animal model rats

(see Methods section). En face analysis of retinal vasculature from NT and non-treated ocular hypertensive rat flat-mounted retina showed that vessel area, percentage area covered by vessels, average vessel length, total vessel length, total junctions, and junction density, which are all parameters reflecting the intactness of the retinal vasculature, were lower in ocular hypertensive rats compared to NT rats, whereas the difference in mean vessel area (NT:  $397,144 \pm 5771 \mu\text{m}$ ; OHT:  $381,317 \pm 13,188 \mu\text{m}$ ;  $P = 0.03$ ) (Fig. 3J) and average vessel length (NT:  $248 \pm 49 \mu\text{m}$ ; OHT:  $177 \pm 27 \mu\text{m}$ ;  $P = 0.005$ ) (Fig. 3D) was statistically significant. Mean lacunarity, which assesses vessel non-uniformity and characterizes oddities found when vasculature organization has been disturbed<sup>41</sup> (higher lacunarity represents a non-uniform organization, with more gaps in the overall vessel pattern/space filling, and lower lacunarity represents a more homogeneous organization, with fewer gaps in overall vessel pattern/space filling), was not significantly changed in ocular hypertensive rats, supporting the suggestion that vessel changes do not result in a significant increase in avascular area (NT:  $0.091 \pm 0.002$ ; OHT:  $0.099 \pm 0.009$ ;  $P = 0.08$ ) (Fig. 3F). These findings support the suggestion that OHT is associated with retinal vasculature impairment. Next, flatmount retina from ocular hypertensive rats treated with NAM in different dosages (200, 400, and 800 mg/kg/d) were analyzed. Mean vessel area ( $P < 0.001$ ) (Fig. 3J), percentage area covered by vessels ( $P = 0.04$ ) (Fig. 3B), total vessel length ( $P = 0.02$ ) (Fig. 3I), total junctions ( $P = 0.01$ ) (Fig. 3H), and junction density ( $P = 0.02$ ) (Fig. 3E), which are used to assess the intactness of the retinal vasculature, were all significantly higher in NAM-treated rats compared to non-treated ocular hypertensive rats in a dose-dependent manner. Similarly, mean lacunarity was significantly lower in NAM-treated rats compared to non-treated ocular hypertensive rats (non-treated OHT:  $0.099 \pm 0.009$ ; NAM [800 mg/kg/d]-treated OHT:  $0.084 \pm 0.002$ ;  $P < 0.001$ ) (Fig. 3F), pointing toward less vascular disorganization in NAM-treated rats compared to non-treated rats. The total number of vessel endpoints (total number of open-ended vessel segments) was significantly higher in NAM-treated ocular hypertensive rats compared to non-treated rats in a dose-dependent manner, possibly representing NAM-triggered sprouting angiogenesis, which could compensate for any vascular dropout caused by OHT (see Discussion section). Complete data are shown in Figure 3.

### Histologic Analysis Revealed Impaired Vessel Integrity Following OHT That was Reduced by NAM Pre Treatment

To determine whether changes to overall vessel morphology were accompanied by a loss of internal structure, we labeled cross-sections of retina and ONH with tight-junction and adherens-junction markers in NT rats, non-treated ocular hypertensive rats, and NAM-treated ocular hypertensive rats. Vessel integrity (antibody-stained vessel lumen wall coverage as a percentage of the total lumen circumference) was quantified in central and peripheral vessels (Figs. 4A, 4B). CD31 integrity was significantly lower in OHT rats compared to NT rats in the central lumen (NT:  $44.93\% \pm 12.926\%$ ; OHT:  $32.74\% \pm 9.041\%$ ;  $P = 0.05$ ) (Fig. 4C) and peripheral blood vessel lumen (for CD31, NT:  $47.44\% \pm 8.491\%$ ; OHT:  $34.22\% \pm 5.946\%$ ;  $P < 0.001$ ) (Fig. 4C).

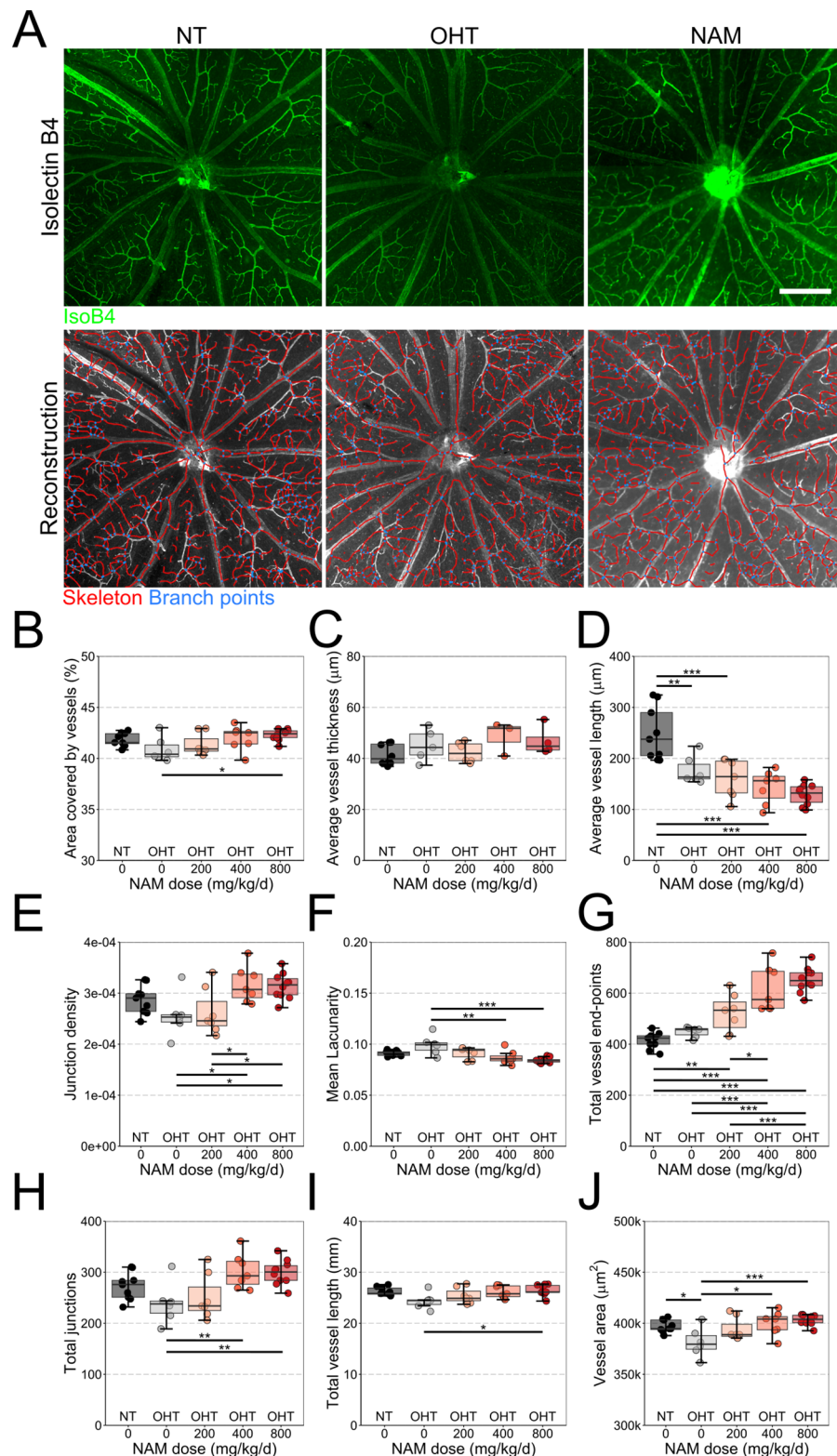


**FIGURE 3.** Vascular remodeling following OHT and protection by NAM. (A) Retinal vasculature was labeled with isolectin B4 to explore vascular changes induced by OHT or NAM treatment. The superficial plexus was imaged to assess vascular morphology (*top row*) ( $n = 9$  NT eyes,  $n = 6$  OHT eyes,  $n = 7$  OHT–NAM 200 mg/kg/d eyes,  $n = 7$  OHT–NAM 400 mg/kg/d eyes, and  $n = 10$  OHT–NAM 800 mg/kg/d eyes). AngioTool was used to reconstruct blood vessels (*bottom row*; red, vessels; blue, junctions). (B–J) OHT induced significant vascular remodeling as indicated in average vessel length and vessel area. In OHT eyes of NAM-treated rats, this remodeling was partially prevented in a dose-dependent manner, as indicated by several AngioTool-specific parameters (area covered by vessels, junction density, total number of junctions, mean lacunarity, total vessel length, and vessel area). Lacunarity is a measure of space filling within the image. High lacunarity indicates less space filling by blood vessels. Scale bar: 400 μm. \* $P < 0.05$ , \*\* $P < 0.01$ , \*\*\* $P < 0.001$ .



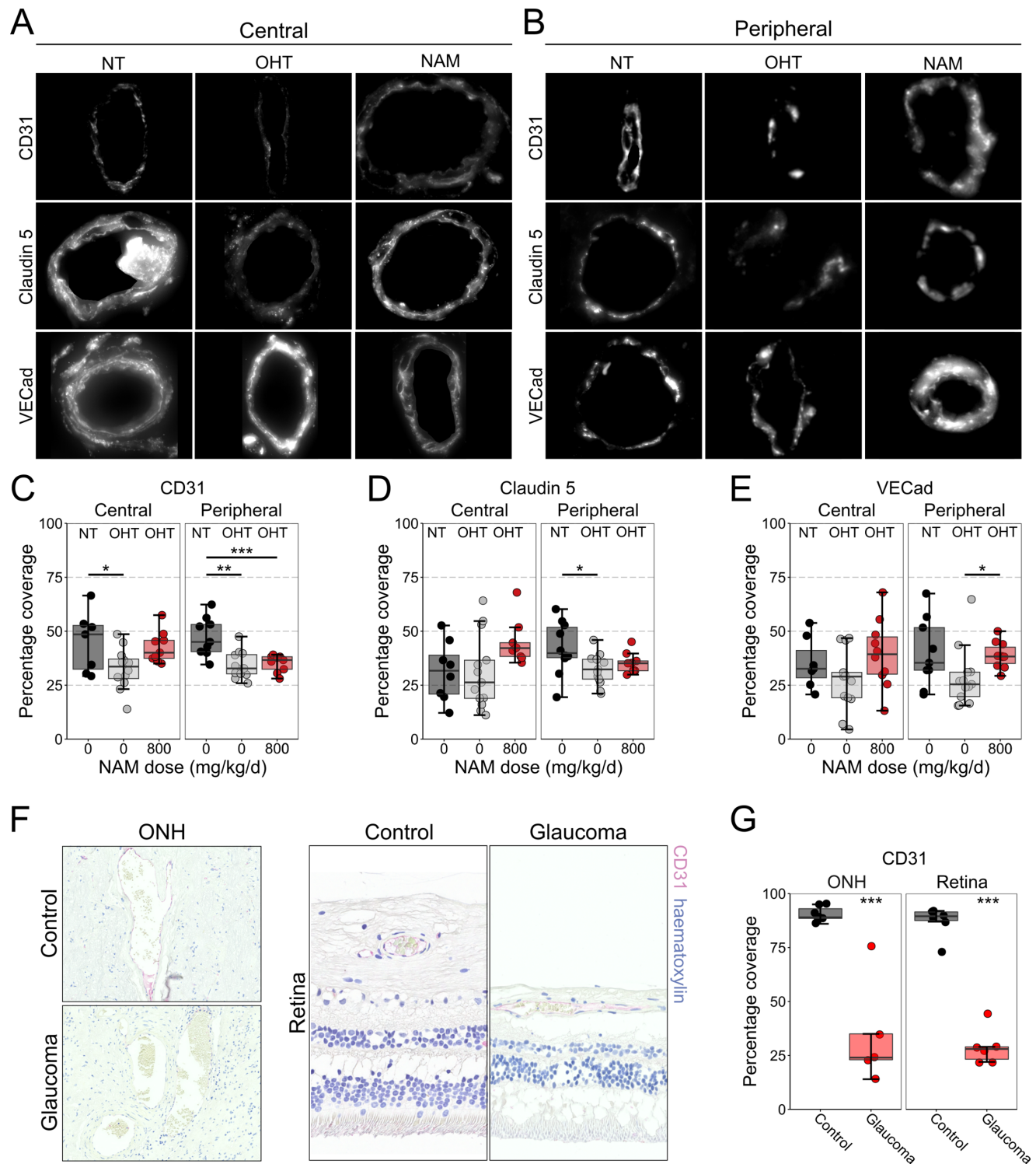


**FIGURE 4.** Loss of vascular integrity following OHT and partial protection by NAM. (A, B) To assess blood vessel integrity in the central and peripheral retina, sections from paraffin-embedded rat eyes were stained with antibodies against CD31, CLDN-5, and VE-cadherin ( $n = 8$  NT eyes,  $n = 12$  OHT eyes, and  $n = 12$  OHT–NAM 800 mg/kg/d eyes). (C–E) OHT induced loss of vascular integrity as assessed by percentage cover of CD31, CLDN-5, and VE-cadherin in central and peripheral vessel walls. NAM treatment partially prevented this remodeling in more peripheral retina. (F) To determine whether this loss is also detectable in human retina, formalin-fixed, paraffin-embedded enucleated eyes from human glaucoma patients ( $n = 6$ ) and non-glaucomatous controls ( $n = 7$ ) were stained with anti-CD31. The percentage cover of CD31 in central and peripheral vessels was significantly reduced in glaucoma (G).

CLDN-5 integrity was significantly reduced in peripheral vessels only (NT:  $42.19\% \pm 11.606\%$ ; OHT:  $32.45\% \pm 6.826\%$ ;  $P = 0.03$ ) (Fig. 4D), and VE-cadherin was unchanged

(central NT:  $35.17\% \pm 11.822\%$ ; OHT:  $27.24\% \pm 13.669\%$ ;  $P = 0.46$ ; peripheral NT:  $39.95\% \pm 15.894\%$ ; OHT:  $28.14\% \pm 13.414\%$ ;  $P < 0.065$ ) (Fig. 4E). In NAM-treated rats, the loss

of CD31 coverage was protected against in central vessels but not in peripheral vessels (central NT:  $44.93\% \pm 12.926\%$ ; OHT-NAM:  $42.68\% \pm 7.324\%$ ;  $P = 0.899$ ; peripheral OHT:  $34.22\% \pm 5.946\%$ ; OHT-NAM:  $35.20\% \pm 3.918\%$ ;  $P = 0.941$ ) (Fig. 4C). CLDN-5 coverage in peripheral vessels was not significantly different from NT or non-treated OHT, suggesting a limited improvement with NAM treatment (Fig. 4D). VE-cadherin coverage in peripheral vessels was higher in NAM-treated rats compared to non-treated ocular hypertensive rats (OHT:  $28.14\% \pm 12.887\%$ ; OHT-NAM:  $38.89\% \pm 5.789\%$ ;  $P < 0.01$ ) (Fig. 4E). Together, these data support partial protection against loss of endothelium integrity and protection against the loss of adherens junctions, supporting mild protection of vascular integrity. Complete data are shown in Figure 4.

In eyes from human glaucoma patients, there was a significantly lower percentage coverage of CD31 in the peripapillary region (control:  $90.43\% \pm 3.457\%$ ; glaucoma:  $34.4\% \pm 24.419\%$ ;  $P < 0.001$ ) (Fig. 4G), as well as the peripheral retina (control:  $87.17\% \pm 7.194\%$ ; glaucoma:  $28.83\% \pm 8.085\%$ ;  $P < 0.001$ ) (Fig. 4G) compared to eyes from controls. This suggest that human glaucoma patients also exhibit impaired vessel integrity. Complete data are shown in Figure 4.

## OCTA CLINICAL TRIAL

### Study Participants

Out of 120 participants included and seen at the baseline visit, 117 completed the study. The participant's clinical characteristics at the baseline visit are shown in Table 1. There were no differences in the prevalence of systemic diseases (systemic arterial hypertension,  $P = 0.60$ ; diabetes mellitus,  $P = 0.50$ ) between the study groups. According to the simplified Hoddaps classification,<sup>32</sup> 36 glaucoma patients (40%) had mild glaucoma, 33 (37%) had moderate glaucoma, and 21 (23%) had severe glaucoma. Patients with PEXG demonstrated a higher mean glaucoma severity than patients with high-tension glaucoma (HTG;  $2.2 \pm 0.8$  compared to  $1.6 \pm 0.7$ ;  $P = 0.01$ ). There were no other significant differences in mean glaucoma severity between the glaucoma groups. The adherence rate for taking NAM treatment according to study protocol was  $>90\%$ . There were no reported serious adverse events. The most common side effect was mild gastrointestinal discomfort of various types, reported in 43 of 117 study participants (37%), including 32 of 87 glaucoma patients (37%) and 10 of 30 healthy controls (33%). While on NAM supplementation, one study participant reported tiredness (NTG), one reported a metallic taste in the mouth (HTG), and one reported heart palpitations (HTG). Three study participants discontinued treatment before the post-treatment visit due to side effects. One study participant in the PEXG group discontinued treatment after two dosages of NAM due to dizziness and light sensitivity, which was likely due to prolonged pharmacologically induced pupil dilation. Two study participants, one from the NTG group and one from the HTG group, discontinued treatment after experiencing gastrointestinal discomfort (the study participant from the HTG group also reported tiredness).

### Changes in OCTA Parameters After NAM Treatment

The control group demonstrated a significant increase after NAM treatment in PD in both the ONH (complete image,  $P = 0.04$ ; inferior quadrant,  $P = 0.01$ ) and the macula

(complete image,  $P = 0.002$ ; inner section,  $P = 0.002$ ; inferior quadrant,  $P = 0.003$ ; nasal quadrant,  $P = 0.02$ ). Glaucoma patients, as a whole, demonstrated a significant increase in PD after NAM treatment only in the temporal quadrant of the macula ( $P = 0.02$ ) (Table 2). Subanalyses showed that glaucoma with severe disease improved in PD after NAM treatment more compared to those with mild or moderate disease. Those with severe glaucoma disease exhibited a significant improvement in PD in both the ONH (inferior quadrant,  $P < 0.05$ ) and the macula (complete image,  $P = 0.02$ ; inner section,  $P = 0.02$ ; superior quadrant,  $P = 0.04$ ; temporal quadrant,  $P = 0.04$ ). In contrast, those with mild disease demonstrated a significant improvement in PD in the superior quadrant of the ONH ( $P < 0.05$ ), and those with moderate disease did not demonstrate any significant improvements in PD after NAM treatment (Supplementary Table S1). Changes in OCT parameters after NAM treatment were analyzed. No significant change was seen in the RNFL between the two visits, but a small but significant decrease was seen in GCL + IPL at the second visit (Supplementary Table S2).

### Changes in IOP After NAM Treatment

When including all participants who completed the study (per protocol analysis), a significant reduction of IOP was seen in the NTG group ( $P = 0.002$ ) and PEXG group ( $P = 0.01$ ). However, when including only participants seen at the same time of day ( $\pm 1$  hour,  $n = 100$ ) in both visits, the IOP reduction was only significant in the NTG group ( $P = 0.002$ ) (Tables 3A, 3B). Multivariate regression analysis, adjusting for glaucoma severity (MD) and diurnal variation between study visits, demonstrated a significant but small positive interaction of prostaglandin analogs and IOP reduction after NAM treatment ( $R^2 = 0.095$ ;  $P = 0.04$ ) (Supplementary Tables S3, S4).

### OCTA at Baseline

Baseline levels of PD and flux index were statistically significantly lower in those with a glaucoma diagnosis compared to controls in all areas analyzed except for the PD in the central macular region. No statistically significant differences in PD or flux index baseline levels between the different glaucoma subtypes were seen (Table 4). Analyses concerning glaucoma severity showed that the PD and flux index baseline levels in the ONH were significantly lower in those with severe disease than those with mild disease in all areas measured. This trend was also seen when comparing mild to moderate and moderate to severe diseases, although statistical significance was not reached for all areas measured. No significant differences were seen when comparing PD baseline levels in the macular region across glaucoma severity groups (Supplementary Table S5).

### Correlations Between OCTA at Baseline and Structure and Function Parameters

Correlation analyses were performed to examine the correlations between vascular parameters (ONH and macula PD and the ONH flux index) and functional (MD) and structural (RNFL and GCL + IPL) parameters in the glaucoma participants. There was a strong positive significant correlation between the complete image ONH PD and MD in both the PEXG group ( $r = 0.632$ ) and the HTG group ( $r = 0.620$ ;  $P <$



TABLE 1. Study Participants' Demographics and Clinical Characteristics

	NTG (n = 30)	HTG (n = 30)	PEXG (n = 30)	Control (n = 30)	P	P					
						NTG vs. Control	HTG vs. Control	PEXG vs. Control	NTG vs. HTG	NTG vs. PEXG	HTG vs. PEXG
Demographic data											
Age (y), mean ± SD	74.5 ± 8.1 15 (50)	74.0 ± 4.2 15 (50)	74.9 ± 5.8 14 (47)	74.0 ± 5.2 14 (47)	0.76	—	—	—	—	—	—
Female sex, n (%)											
Ophthalmologic data											
IOP (mmHg), mean ± SD	11.3 ± 2.5 17 (57)	13.9 ± 3.3 9 (30)	14.1 ± 3.9 19 (63)	13.6 ± 3.6 4 (13)	0.004* <0.001*	0.056 —†	1 —†	1 —†	0.02* —†	0.008* —†	1 —†
Pseudophakia, n (%)	0 (0)	0 (0)	30 (100)	2 (7)	<0.001*	—‡	—‡	—‡	—‡	—‡	—‡
PEX, n (%)	—	—	—	—	—	—	—	—	—	—	—
MD (dB), mean ± SD	−8.4 ± 5.2 81/15	−6.4 ± 4.1 88/21	−12.0 ± 7.7 69/38	0.3 ± 1.0 99/2	0.008* 0.009*	—	—	—	0.43 0.45	0.31 0.32	0.006* 0.007*
VFI (%), median/IQR	67.0 ± 7.4 (23)	61.9 ± 8.3 (22)	61.7 ± 5.0 (26)	87.7 ± 6.7 (29)	<0.001*	<0.001*	<0.001*	<0.001*	0.09	0.05	1
RNFL (μm), mean ± SD	59.9 ± 8.5 (25)	62.4 ± 7.4 (30)	57.8 ± 6.4 (30)	74.4 ± 5.8 (25)	<0.001*	<0.001*	<0.001*	<0.001*	1	1	0.10
GCL + IPL (μm), mean ± SD											
Anti-glaucoma eye drops, n (%)											
Beta-blockers	20 (67)	20 (67)	13 (43)	—	0.132	—	—	—	—	—	—
Prostaglandin analogs	25 (83)	24 (80)	20 (67)	—	0.379	—	—	—	—	—	—
Alpha-2 agonists	4 (13)	3 (10)	2 (7)	—	0.905	—	—	—	—	—	—
Carbonic anhydrase inhibitors	12 (40)	10 (33)	8 (27)	—	0.597	—	—	—	—	—	—
Cholinergic agents	0 (0)	0 (0)	1 (3)	—	1	—	—	—	—	—	—
No. of anti-glaucoma eye drops, mean ± SD	2.0 ± 1.1	1.9 ± 1.0	1.5 ± 1.3	—	0.124	—	—	—	—	—	—

Statistically significant findings are presented in bold.

\* P < 0.05.

† Post hoc test was performed by calculating the adjusted standardized residuals and converting these into P values. Bonferroni correction was used to adjust for type I error inflation. Significance after correction was set to P < 0.00625. Control and PEXG were significant; NTG and HTG were not.

‡ Post hoc test was performed by calculating the adjusted standardized residuals and converting these into P values. Bonferroni correction was used to adjust for type I error inflation. Significance after correction was set to P < 0.00625. Control, PEXG, NTG, and HTG were significant.

TABLE 2. Change in OCTA Parameters After Nicotinamide Treatment

	Mean ± SD (n)				Control	P				
	NTG	HTG	PEXG	Glaucoma, Total		NTG	HTG	PEXG	Control	Glaucoma, Total
ONH Angiography										
Change in PD (%)										
Complete	0.2 ± 1.2 (29)	0.3 ± 1.2 (28)	< -0.1 ± 1.3 (27)	0.2 ± 1.4 (84)	0.7 ± 1.7 (29)	0.49	0.23	0.85	<b>0.04*</b>	0.15
Superior	0.4 ± 1.8 (29)	0.2 ± 1.7 (28)	0.2 ± 1.5 (27)	0.3 ± 1.6 (84)	0.6 ± 1.6 (29)	0.26	0.47	0.06	0.41	0.11
Inferior	0.1 ± 1.6 (29)	0.2 ± 1.5 (28)	0.2 ± 1.7 (26)	0.1 ± 1.5 (83)	0.8 ± 1.6 (29)	0.82	0.60	0.55	<b>0.01*</b>	0.43
Nasal	-0.1 ± 1.9 (29)	< 0.1 ± 1.6 (28)	< -0.1 ± 2.0 (27)	< -0.1 ± 1.8 (84)	0.6 ± 2.2 (29)	0.84	0.95	0.96	0.20	0.90
Temporal	0.2 ± 1.7 (29)	0.6 ± 2.0 (28)	- 0.5 ± 1.9 (27)	0.1 ± 1.9 (84)	0.6 ± 2.7 (29)	0.69	0.11	0.15	0.24	0.54
Change in flux index (%)										
Complete	0.002 ± 0.020 (29)	0.001 ± 0.020 (28)	< -0.001 ± 0.022 (27)	0.001 ± 0.021 (84)	0.003 ± 0.033 (29)	0.51	0.61	0.73	0.61	0.65
Macula Angiography										
Change in PD (%)										
Central	0.2 ± 3.0 (25)	0.7 ± 2.7 (29)	0.8 ± 2.8 (25)	0.6 ± 2.8 (79)	1.0 ± 2.7 (30)	0.70	0.21	0.14	0.12	0.07
Inner	0.2 ± 2.5 (25)	0.6 ± 2.1 (29)	0.6 ± 1.6 (25)	0.4 ± 2.1 (79)	1.0 ± 1.7 (30)	0.76	0.15	0.05	<b>0.002*</b>	0.11
Complete	0.2 ± 2.5 (25)	0.6 ± 2.2 (29)	0.7 ± 1.6 (25)	0.6 ± 2.3 (79)	1.0 ± 1.7 (30)	0.71	0.15	0.07	<b>0.002*</b>	0.09
Superior	0.4 ± 2.6 (25)	0.1 ± 2.2 (29)	1.0 ± 2.5 (25)	0.5 ± 2.4 (79)	0.4 ± 3.3 (30)	0.41	0.76	0.06	0.47	0.07
Inferior	-0.6 ± 3.7 (25)	1.2 ± 3.5 (29)	0.2 ± 3.0 (25)	0.3 ± 3.4 (79)	1.6 ± 2.6 (30)	0.15	0.07	0.70	<b>0.003*</b>	0.76
Nasal	0.6 ± 3.0 (25)	0.2 ± 3.0 (29)	0.2 ± 3.1 (25)	0.3 ± 3.0 (79)	1.2 ± 3.4 (30)	0.36	0.71	0.70	<b>0.02*</b>	0.33
Temporal	0.3 ± 3.3 (25)	0.8 ± 2.4 (29)	1.1 ± 2.3 (25)	0.7 ± 2.7 (79)	0.9 ± 3.6 (30)	0.66	0.08	<b>0.03*</b>	0.24	<b>0.02*</b>

Statistically significant findings are presented in bold.  
\* P < 0.05.

**TABLE 3A.** IOP at Baseline and After Nicotinamide Treatment (All Participants)

	<i>n</i>	IOP (mmHg), Mean (SD)			<i>P</i>
		Baseline	Posttreatment	Difference	
NTG	29	11.3 (2.5)	10.3 (2.4)	1.0 (1.4)	<b>0.002*</b>
HTG	29	13.8 (3.3)	13.7 (4.1)	0.2 (2.4)	0.70
PEXG	29	14.3 (3.9)	13.1 (3.0)	1.2 (2.5)	<b>0.01*</b>
Glaucoma, total	87	13.2 (3.5)	12.4 (3.5)	0.8 (2.2)	<b>&lt;0.001*</b>
Control	30	13.6 (3.6)	13.2 (2.9)	0.4 (1.8)	0.28
All participants	117	13.3 (3.5)	12.6 (3.4)	0.7 (2.1)	<b>&lt;0.001*</b>

Statistically significant findings are presented in bold.

\*  $P < 0.05$ .

**TABLE 3B.** IOP at Baseline and After Nicotinamide Treatment (Only Participants With Diurnal Variation  $\leq 1$  Hour Between Visits)

Cohort	<i>n</i>	IOP (mmHg), Mean (SD)			<i>P</i>
		Baseline	Posttreatment	Difference	
NTG	29	11.3 (2.5)	10.3 (2.4)	1.0 (1.4)	<b>0.002*</b>
HTG	28	13.6 (3.2)	13.4 (3.9)	0.3 (2.4)	0.59
PEXG	20	13.2 (3.4)	12.3 (3.0)	0.9 (2.2)	0.09
Glaucoma, total	77	12.7 (3.2)	12.0 (3.4)	0.7 (2.0)	<b>0.004*</b>
Control	23	13.9 (3.1)	13.2 (2.4)	0.7 (1.7)	0.06
All participants	100	12.9 (3.2)	12.3 (3.3)	0.7 (1.9)	<b>&lt;0.001*</b>

Statistically significant findings are presented in bold.

\*  $P < 0.05$ .

0.001 for both) and a moderate positive significant correlation in the NTG group ( $r = 0.464$ ;  $P = 0.01$ ). In addition, the HTG group demonstrated a strong positive significant correlation between the complete image ONH flux index and MD ( $r = 0.679$ ;  $P < 0.001$ ) and a moderate positive significant correlation between the complete image macula PD and MD ( $r = 0.393$ ;  $P = 0.03$ ). No other significant correlations were seen between PD and MD.

The HTG group demonstrated a strong positive significant correlation between the complete image ONH PD and RNFL ( $r = 0.621$ ;  $P = 0.002$ ), a moderate positive correlation between the complete image ONH PD and GCL + IPL ( $r = 0.421$ ;  $P = 0.02$ ), a moderate positive correlation between the complete image macula PD and RNFL ( $r = 0.469$ ;  $P = 0.03$ ), and a moderate positive correlation between the complete image macula PD and GCL + IPL ( $r = 0.479$ ;  $P = 0.007$ ). Patients with NTG showed a strong positive correlation between the complete image ONH PD and GCL + IPL ( $r = 0.549$ ;  $P = 0.004$ ). No other significant correlations were found between PD and the structural parameters RNFL and GCL + IPL.

### Topical Glaucoma Medications and Systemic Arterial Hypertension Related to the Effect of NAM Treatment on OCTA Parameters

Glaucoma participants were subanalyzed based on topical glaucoma medications and systemic arterial hypertension, and several significant results were found when looking at the effect of NAM treatment on PD (Supplementary Tables S6–S20). To assess the possible effects of topical glaucoma medications, multivariate regression analyses were performed, adjusting for glaucoma severity (MD). The multivariate regression analyses demonstrated a significant but small negative interaction of prostaglandin analogs and the effect of NAM treatment on PD in the central macular

region ( $R^2 = 0.082$ ;  $P = 0.04$ ). In addition, to assess the possible effects of systemic arterial hypertension, multivariate regression analyses adjusting for age were performed and demonstrated a significant but small negative interaction between systemic arterial hypertension and the effect of NAM treatment on PD in the ONH complete image ( $R^2 = 0.067$ ;  $P = 0.02$ ).

Taken together, these data demonstrate that vascular dysfunction occurs in glaucoma, with vasoprotection provided by NAM.

## DISCUSSION

NAM is profoundly neuroprotective in animal models of glaucoma. The proposed mechanism is the prevention of neurodegeneration via replenishment of retinal NAD<sup>6</sup> and modulation of metabolic and mitochondrial function.<sup>6,33</sup> However, NAM also has known vasoactive properties,<sup>28</sup> and mounting evidence suggests that glaucoma is associated with impairment of the retinal vasculature.<sup>9</sup> In this study, we sought to investigate if NAM could improve retinal vasculature, which has never been explored before, to the best of our knowledge. This is important in the context of ongoing glaucoma clinical trials using NAM, as it helps define the effects of NAM and whether the retinal vasculature should be assessed in glaucoma patients on NAM.

To address these concerns, we investigated retinal tissue from ocular hypertensive and healthy rats via histopathology and with a number of imaging-based software tools. We analyzed the retinal tissue using AngioTool, a publicly available software designed for the reproducible quantification of vascular networks in microscopic images. AngioTool identifies vascular configurations according to preset parameters. Our analysis revealed a decrease in a number of parameters representing intactness of the retinal vasculature (vessel area, percentage area covered by vessels, average vessel length, total vessel length, total junctions, and junction density) in ocular hypertensive rats compared to NT controls. In NAM-treated rats, many of these parameters showed less of a decrease compared to non-treated rats in a dose-dependent manner. These findings suggest that the integrity and organization of the retinal vasculature are disturbed in ocular hypertension/glaucoma and that NAM treatment may protect against these alterations in a dose-dependent manner. Furthermore, we identified an increase in total vessel endpoints (total open-ended vessel segments) in NAM-treated ocular hypertensive rats compared to non-treated rats, in a dose-dependent manner. Previous studies have shown that NAM promotes angiogenesis by rescuing renewal capacities in endothelial cells.<sup>42,43</sup> It is conceivable that our findings represent an increase in sprouting angiogenesis compensating for the continuous vascular dropout caused by OHT, which could point toward a possible mechanism by which NAM prevents vascular rarefaction and disintegration, but this cannot be conclusively determined based on the present data. Furthermore, it appears plausible that NAM may exert a booster effect on compensating angiogenesis only in conditions of extreme vascular dropout (that were present in the ocular hypertensive rats yet would not be present in medically attended glaucoma patients) and only in very high dosages (that the rats received but would not be tolerable in patients with glaucoma).

For histopathology, we stained the retinal tissue against proteins that are commonly associated with maintaining endothelial junctions and retinal blood barrier



TABLE 4. Baseline Levels of OCTA Parameters

	Mean ± SD (n)				P							
	NTG	HTG	PEXG	Control	P	NTG vs.		NTG vs.		HTG vs.	PEXG	
						Control	Control	Control	Control			
PD (%)	ONH Angiography											
	Complete	39.2 ± 2.4 (30)	39.1 ± 2.2 (29)	38.3 ± 2.8 (28)	44.7 ± 1.5 (29)	<0.001*	<0.001*	<0.001*	1	0.94	1	
	Superior	36.7 ± 4.2 (30)	37.0 ± 3.1 (29)	35.3 ± 4.2 (28)	44.1 ± 2.0 (29)	<0.001*	<0.001*	<0.001*	1	0.77	0.50	
	Inferior	35.2 ± 3.3 (30)	36.1 ± 3.9 (29)	35.1 ± 4.0 (27)	44.7 ± 2.2 (29)	<0.001*	<0.001*	<0.001*	1	1	1	
	Nasal	41.2 ± 2.9 (30)	40.3 ± 3.0 (29)	39.7 ± 3.6 (28)	43.8 ± 2.2 (28)	<0.001*	0.006*	<0.001*	1	0.40	1	
Temporal	43.2 ± 3.1 (30)	43.0 ± 2.6 (29)	42.5 ± 2.7 (28)	46.1 ± 2.3 (29)	<0.001*	<0.001*	<0.001*	1	1	1		
Flux index (%)												
Complete	0.348 ± 0.036 (30)	0.367 ± 0.029 (29)	0.355 ± 0.039 (28)	0.432 ± 0.033 (29)	<0.001*	<0.001*	<0.001*	0.19	1	1		
PD (%)	Macula Angiography											
	Central	20.3 ± 6.6 (26)	20.5 ± 6.1 (30)	19.1 ± 6.7 (26)	21.7 ± 5.4 (30)	0.51	—	—	—	—	—	
	Inner	38.6 ± 3.2 (26)	39.8 ± 2.3 (30)	39.8 ± 2.1 (26)	41.6 ± 1.9 (30)	<0.001*	<0.001*	0.02*	0.01*	1	1	
	Complete	36.5 ± 3.3 (26)	37.6 ± 2.4 (30)	37.5 ± 2.4 (26)	39.3 ± 1.7 (30)	<0.001*	0.001*	0.03*	0.01*	1	1	
	Superior	39.1 ± 3.7 (26)	40.2 ± 2.4 (30)	39.2 ± 2.8 (26)	41.8 ± 2.7 (30)	0.001*	0.01*	0.10	0.002*	1	1	
	Inferior	38.0 ± 3.2 (26)	38.9 ± 3.4 (30)	39.6 ± 3.2 (26)	41.1 ± 2.3 (30)	0.006*	0.003*	0.13	0.45	1	0.62	
	Nasal	39.1 ± 4.3 (26)	40.6 ± 2.6 (30)	40.7 ± 2.7 (26)	41.9 ± 2.6 (30)	0.01*	0.007*	0.11	0.32	1	1	
Temporal	38.1 ± 3.8 (26)	39.5 ± 2.7 (30)	39.7 ± 3.0 (26)	41.5 ± 2.9 (30)	<0.001*	<0.001*	0.01*	0.05	1	0.98		

Statistically significant findings are presented in bold.

\* P < 0.05.

integrity: CD31, CLDN-5, and VE-cadherin. Our analysis revealed significant loss of integrity in tissue from ocular hypertensive rats, with mild protection against this in NAM-treated rats. Because this initial study was based on an animal model of glaucoma, it was unclear to what extent the results apply to glaucoma patients. To support our data, we utilized ocular tissue from glaucoma patients for another histopathology analysis with anti-CD31 staining, again demonstrating reduced CD31 immunoreactivity levels in optic nerve heads and peripheral retina. For our histopathology study, we used ocular tissue exclusively from rats and patients with end-stage glaucoma for matching reasons and because we aimed to investigate the long-term effect of NAM on retinal vasculature, given its known long-term neuroprotective effect. Thus, whether our histopathology findings represent a loss of CD31 protein or generalized blood vessel loss cannot be conclusively determined based on the available data. Further research is warranted to specify if CD31 loss occurs simultaneously with general retinal blood vessel loss or if it is a precursor of it.

Given these promising basic scientific results, we next assessed the retinal vasculature in a cohort of patients with POAG, NTG, and PEXG, as well as age- and sex-matched healthy controls, using OCTA. Glaucoma patients from the POAG, NTG, and PEXG subgroups were included because they all likely have different pathophysiological mechanisms, including the role of vascular impairment, and, therefore, may respond differently to NAM treatment. In our patients, the PD in the ONH and macula were significantly lower in glaucoma compared to age- and sex-matched healthy controls in all measured areas except the central region of the macula. However, although not significant, PD in the central region of the macula was lower in glaucoma compared to controls ( $20.0\% \pm 6.4\%$  vs.  $21.7\% \pm 5.4\%$ ;  $P = 0.21$ ). Overall, the results of our animal, histopathological, and OCTA-based studies strongly support the concept of retinal vascular compromise as an important aspect in the etiopathogenesis of glaucoma.

A recent study has shown that it is possible to improve retinal vasculature in patients with glaucoma with short-term pharmacological treatment.<sup>44</sup> After this short-term NAM treatment, PD in the complete macula and ONH area in healthy controls and the temporal quadrant of the macula in glaucoma patients was significantly improved. In patients with glaucoma, the effect of NAM on the retinal vasculature was correlated with the participants' current topical glaucoma medications, systemic hypertension, and glaucoma disease severity.

In this study, the healthy controls demonstrated increased PD after NAM treatment in the complete image of ONH and macula. In contrast, the glaucoma group demonstrated an increase in the temporal quadrant of the macula. A possible explanation could be that the vasculature of glaucoma-affected eyes has an impaired physiologic reactivity to metabolic and pharmacologic triggers such as NAM, whereas healthy control eyes still possess that capacity. This theory is supported by previous evidence demonstrating an attenuated vasodilatation in glaucoma patients compared to healthy controls following endothelin-A (ET<sub>A</sub>) receptor antagonism.<sup>45</sup> In contrast, the PD after NAM treatment increased more in those with severe glaucoma compared to mild and moderate glaucoma. One possible explanation for this is different susceptibility to NAM treatment in participants depending on genotype. Another possibility is that the number and type of anti-glaucoma eye drops participants

were on during the study biased analysis of the PD increase after NAM treatment based on glaucoma severity. There was a significant association between glaucoma severity and the number of anti-glaucoma eye drops when stratified to either "low medication" (0 or 1 eye drops) or "high medication" (2–4 eye drops) ( $P = 0.02$ ). There was also a significant association between glaucoma severity and specific types of anti-glaucoma eye drops, including prostaglandin analogs ( $P = 0.006$ ) and carbonic anhydrase inhibitors ( $P = 0.03$ ). Further studies are therefore needed to investigate what factors influence the retinal vascular effects following NAM treatment.

After 2 weeks of NAM treatment, no change was seen in RNFL (as measured by OCT), but a small but significant decrease was seen in GCL + IPL thickness. This small reduction is not likely to be of clinical significance, and it is unlikely that clinically detectable RGC death could have occurred over the short time frame of the study. However, this decrease in GCL + IPL thickness supports our findings that increased blood flow after NAM measured with OCTA is independent of a potential change in OCT thickness, as a decrease in OCT should rather diminish the findings than explain them. The absence of an increase in OCT parameters supports that the OCTA results are not a false positive.

In our rat studies, the vasoprotective effects of NAM were strong, yet the effect sizes seen in the clinical trial with the human glaucoma patients were small. This difference may be explained by the fact that, in the rats, NAM treatment was prophylactic. At the same time, the human patients had long-lasting glaucoma before inclusion into the clinical trial; thus, their retinal vasculature had been compromised long before the NAM treatment. It appears more plausible that NAM can prevent vascular damage from occurring rather than reverse it. Furthermore, the treatment duration of 2 weeks was short for humans, and the findings may not be directly comparable with the results of the animal study, considering the rats' much shorter life cycles.

Although the changes in retinal vasculature seen in our patients were small, and the clinical relevance hence may be limited, our findings still indicate that NAM may exert beneficial effects on the retinal vasculature in pre-existing glaucoma. It is conceivable that NAM would be even more beneficial if treatment were started earlier in the course of the disease and if the treatment duration was longer.

NAM is known to attenuate vasoconstriction through its inhibitory actions on ADP-ribosyl cyclase (ADPRC).<sup>28</sup> The vasoconstrictive effects of endothelin are mediated via ADPRC.<sup>28</sup> Endothelin signaling has been hypothesized to play a role in vascular impairment associated with glaucoma. ET-1 is widely distributed in ocular tissues, including the retina and ONH.<sup>46</sup> In patients with glaucoma, ET-1 levels in the aqueous humor<sup>47</sup> and plasma<sup>48</sup> are higher than in healthy controls. Short-term treatment with a mixed ET<sub>A</sub> and ET<sub>B</sub> receptor antagonist increased ocular blood flow in patients with glaucoma and healthy subjects.<sup>49</sup> In a recent study, increased plasma levels of ET-1 correlated negatively with peripapillary and macula vessel density in patients with glaucoma as measured by OCTA.<sup>25</sup> One plausible explanation for the improvements in the retinal vasculature seen in our clinical trial could be the inhibitory effects of NAM on endothelin-mediated vasoconstriction. Furthermore, in animal models, intravitreal injection of ET-1 was sufficient to drive RGC death,<sup>50,51</sup> and the administration of an ET<sub>A</sub> and ET<sub>B</sub> receptor antagonist protected from glaucoma.<sup>26</sup> Importantly, a recent study using the DBA/2J mouse model of

inherited glaucoma showed that deletion of  $ET_A$  from retinal vascular mural cells prevented ET-1-mediated vasoconstriction and RGC death.<sup>27</sup> Inhibition of endothelin-mediated vasoconstriction may therefore have neuroprotective effects in glaucoma. Although NAM appears to protect from vascular endothelial dropout in the animal model (as demonstrated by histopathological analysis using antibody-staining against CD31, CLDN-5, and VE-cadherin, proteins that are commonly associated with vascular endothelial integrity), vascular morphological changes in humans after only 2 weeks of NAM treatment appear implausible. Likely, the increase in retinal vascular parameters as seen in our OCTA analysis represents an enhancement of retinal perfusion due to vasodilation, possibly via the above-mentioned mechanism, and increased cardiovascular activity. Unfortunately, it is impossible to histopathologically analyze the ocular tissue from our patients; hence, at the present time we can only note that following NAM treatment there is less vascular endothelial dropout in the ocular hypertensive animal model and at the same time an increase in retinal perfusion in our glaucoma patients, yet we cannot determine if there is any link between these observations apart from the NAM treatment.

In the central macular region, a small but significant negative interaction of prostaglandin analogs and the effect of NAM treatment on PD was seen, and, in the macular complete and inner region, there was a trend that participants who were not on prostaglandin analogs demonstrated a better effect of NAM treatment. Studies have shown that treatment with prostaglandin analogs can improve retinal vessel density.<sup>52,53</sup> Moreover, topical administration of prostaglandin analogs inhibits ET-1-induced decreases in ONH blood flow in animals.<sup>54</sup> NAM can reverse ET-1-mediated vasoconstriction.<sup>28</sup> Thus, a possible explanation for the better effect on macular PD after NAM treatment in participants not on prostaglandin analogs seen in this study could be competing vasoactive mechanisms between prostaglandin analogs and NAM.

A small (0.8 mmHg) but significant reduction of IOP after short-term treatment with NAM was seen in this study when including all glaucoma patients. This finding mirrors a similar significant (but small, 1.2 mmHg) reduction in IOP in NAM-treated NT rats as previously demonstrated.<sup>33</sup> Subanalyses revealed that the NTG and PEXG patients demonstrated significant IOP reductions (1.0 mmHg and 1.2 mmHg, respectively), but the HTG patients did not. As IOP varies throughout the day,<sup>55</sup> subanalyses were performed that included only participants seen at the same time of day ( $\pm 1$  hour) in both visits, with only the NTG patients still exhibiting a significant IOP reduction. Multivariate regression analyses demonstrated that treatment with prostaglandin analogs was associated with a greater IOP reduction after NAM treatment. NTG and PEXG patients on prostaglandin analogs demonstrated a significant reduction in IOP, and the significance remained after analyzing only those seen at the same time of day ( $\pm 1$  hour). Contrary to the results seen in this study, Hui et al.<sup>22</sup> found no evidence of IOP reduction in patients with glaucoma after 6 weeks of NAM treatment. A possible explanation for this discrepancy may be that IOP measurements in this study, as for the PEXG patients and the controls, were done with three different rebound tonometers by two different operators. Thus, inter-device and interoperator variability is a possible confounder of the results.<sup>56–58</sup> In contrast to this current study, Hui et al.<sup>22</sup> performed no separate analyses on subgroups based on

glaucoma subtype or topical glaucoma medications, such as prostaglandin analogs, which could be a plausible explanation for the different results seen in the studies. It has been shown that a placebo effect commonly occurs in glaucoma clinical trials<sup>59</sup>; thus, expectations of NAM to have positive effects may also have contributed to the IOP reduction seen in this current study. Further studies are needed to establish the possible effects of NAM on IOP in patients with glaucoma.

This study has several strengths. First, there were no significant differences in age, gender, systemic arterial hypertension, or diabetes mellitus among any of the study groups, and these factors have been shown to influence the retinal vasculature measured using OCTA.<sup>60</sup> Second, all OCTA scans had a signal strength of 9 or above, and all posttreatment OCTA scans were acquired using the inbuilt “track to prior scan” option.<sup>38–40</sup> Third, the adherence rate to NAM treatment was  $>90\%$  in all participants who completed the study. Our study is limited by the lack of registration of factors that may have been shown to influence OCTA parameters, such as heart rate, mean arterial blood pressure, recent exercise, and myopia.<sup>10,61</sup> Thus, the measurements were not adjusted for this in the analyses. Regarding the NAM treatment, the adherence rate was checked by asking each participant, but patients tend to conceal nonadherence.<sup>62</sup> Therefore, solely having relied on the participant's information about their adherence rate may constitute a limitation.

In conclusion, treatment with NAM can limit retinal vascular damage in an animal model of glaucoma. In addition, short-term NAM treatment in patients with pre-existing glaucoma can yield an increase in retinal vessel parameters. However, the improvements were small and of limited clinical relevance. Thus, we find it less likely that the neuroprotective effects of NAM in glaucoma seen in recent preclinical<sup>20,21,33</sup> and clinical<sup>22,23</sup> trials are due to the vasoactive properties of NAM. Importantly, no negative effects on the retinal vasculature were seen with NAM treatment. Topical glaucoma medications, particularly prostaglandin analogs, and systemic arterial hypertension may influence the effect of NAM treatment. Although the effect size is small, this might be worth considering for the ongoing clinical trials for glaucoma where IOP-lowering treatment is still administered and for future stratification of patients onto NAM treatment.

### Acknowledgments

The authors thank St. Erik Eye Hospital for financial support for the research and clinical histopathology space and Umeå University Hospital for financial research support.

Supported by Karolinska Institutet in the form of a Board of Research Faculty Funded Career Position, by St. Erik Eye Hospital philanthropic donations, and by grants from Vetenskaprådet (2018-02124 and 2022-00799) and Ögonfonden (PAW). Additional support was provided through regional agreements between Umeå University and Västerbotten County Council and by grants from Alice and Knut Wallenberg Foundation, Crown Princess Margareta's Foundation, Ögonfonden, Cronqvist Foundation, and the Swedish Medical Society Foundation (GJ). The funding organizations had no role in the design or conduct of this research.

Disclosure: **S.T. Gustavsson**, None; **T.J. Enz**, None; **J.R. Tribble**, None; **M. Nilsson**, None; **A. Lindqvist**, None; **C. Lindén**, None; **A. Hagström**, None; **C. Rutigliani**, None; **E. Lardner**, None;



G. Stålhammar, None; P.A. Williams, P; G. Jóhannesson, Abbvie (C), Alcon (C), Oculis (C), Santen (C), Thea (C)

## References

1. Tham YC, Li X, Wong TY, Quigley HA, Aung T, Cheng CY. Global prevalence of glaucoma and projections of glaucoma burden through 2040: a systematic review and meta-analysis. *Ophthalmology*. 2014;121(11):2081–2090.
2. Leske MC, Heijl A, Hyman L, et al. Predictors of long-term progression in the early manifest glaucoma trial. *Ophthalmology*. 2007;114(11):1965–1972.
3. Peters D, Bengtsson B, Heijl A. Lifetime risk of blindness in open-angle glaucoma. *Am J Ophthalmol*. 2013;156(4):724–730.
4. Casson RJ, Chidlow G, Crowston JG, Williams PA, Wood JPM. Retinal energy metabolism in health and glaucoma. *Prog Retin Eye Res*. 2021;81:100881.
5. Tribble JR, Vasalauskaitė A, Redmond T, et al. Midget retinal ganglion cell dendritic and mitochondrial degeneration is an early feature of human glaucoma. *Brain Commun*. 2019;1(1):fcz035.
6. Williams PA, Harder JM, Foxworth NE, et al. Vitamin B<sub>3</sub> modulates mitochondrial vulnerability and prevents glaucoma in aged mice. *Science*. 2017;355(6326):756–760.
7. Tribble JR, Harder JM, Williams PA, John SWM. Ocular hypertension suppresses homeostatic gene expression in optic nerve head microglia of DBA/2 J mice. *Mol Brain*. 2020;13(1):81.
8. Williams PA, Harder JM, John SWM. Glaucoma as a metabolic optic neuropathy: making the case for nicotinamide treatment in glaucoma. *J Glaucoma*. 2017;26(12):1161–1168.
9. Chan KKW, Tang F, Tham CCY, Young AL, Cheung CY. Retinal vasculature in glaucoma: a review. *BMJ Open Ophthalmol*. 2017;1(1):e000032.
10. Mannil SS, Agarwal A, Conner IP, Kumar RS. A comprehensive update on the use of optical coherence tomography angiography in glaucoma. *Int Ophthalmol*. 2023;43(5):1785–1802.
11. Moghimi S, Zangwill LM, Penteadó RC, et al. Macular and optic nerve head vessel density and progressive retinal nerve fiber layer loss in glaucoma. *Ophthalmology*. 2018;125(11):1720–1728.
12. Pradhan ZS, Dixit S, Sreenivasiah S, et al. A sectoral analysis of vessel density measurements in perimetrically intact regions of glaucomatous eyes: an optical coherence tomography angiography study. *J Glaucoma*. 2018;27(6):525–531.
13. Yarmohammadi A, Zangwill LM, Diniz-Filho A, et al. Peripapillary and macular vessel density in patients with glaucoma and single-hemifield visual field defect. *Ophthalmology*. 2017;124(5):709–719.
14. Chen CL, Bojikian KD, Wen JC, et al. Peripapillary retinal nerve fiber layer vascular microcirculation in eyes with glaucoma and single-hemifield visual field loss. *JAMA Ophthalmol*. 2017;135(5):461–468.
15. Hou H, Moghimi S, Kamalipour A, et al. Macular thickness and microvasculature loss in glaucoma suspect eyes. *Ophthalmol Glaucoma*. 2022;5(2):170–178.
16. Wang J, He Z. NAD and axon degeneration: from the Wlds gene to neurochemistry. *Cell Adh Migr*. 2009;3(1):77–87.
17. Lautrup S, Sinclair DA, Mattson MP, Fang EF. NAD<sup>+</sup> in brain aging and neurodegenerative disorders. *Cell Metab*. 2019;30(4):630–655.
18. Jadeja RN, Thounaojam MC, Bartoli M, Martin PM. Implications of NAD<sup>+</sup> metabolism in the aging retina and retinal degeneration. *Oxid Med Cell Longev*. 2020;2020:2692794.
19. Williams PA, Harder JM, Foxworth NE, Cardozo BH, Cochran KE, John SWM. Nicotinamide and WLD<sup>S</sup> act together to prevent neurodegeneration in glaucoma. *Front Neurosci*. 2017;11:232.
20. Williams PA, Harder JM, Cardozo BH, Foxworth NE, John SWM. Nicotinamide treatment robustly protects from inherited mouse glaucoma. *Commun Integr Biol*. 2018;11(1):e1356956.
21. Chou TH, Romano GL, Amato R, Porciatti V. Nicotinamide-rich diet in DBA/2J mice preserves retinal ganglion cell metabolic function as assessed by PERG adaptation to flicker. *Nutrients*. 2020;12(7):1910.
22. Hui F, Tang J, Williams PA, et al. Improvement in inner retinal function in glaucoma with nicotinamide (vitamin B<sub>3</sub>) supplementation: a crossover randomized clinical trial. *Clin Exp Ophthalmol*. 2020;48(7):903–914.
23. De Moraes CG, John SWM, Williams PA, Blumberg DM, Cioffi GA, Liebmann JM. Nicotinamide and pyruvate for neuroenhancement in open-angle glaucoma: a phase 2 randomized clinical trial. *JAMA Ophthalmol*. 2022;140(1):11–18.
24. Thai TL, Fellner SK, Arendshorst WJ. ADP-ribosyl cyclase and ryanodine receptor activity contribute to basal renal vasomotor tone and agonist-induced renal vasoconstriction in vivo. *Am J Physiol Renal Physiol*. 2007;293(4):F1107–F1114.
25. Lommatzsch C, Rothaus K, Schopmeyer L, et al. Elevated endothelin-1 levels as risk factor for an impaired ocular blood flow measured by OCT-A in glaucoma. *Sci Rep*. 2022;12(1):11801.
26. Howell GR, MacNicol KH, Braine CE, et al. Combinatorial targeting of early pathways profoundly inhibits neurodegeneration in a mouse model of glaucoma. *Neurobiol Dis*. 2014;71:44–52.
27. Marola OJ, Howell GR, Libby RT. Vascular derived endothelin receptor A controls endothelin-induced retinal ganglion cell death. *Cell Death Discov*. 2022;8(1):207.
28. Thai TL, Arendshorst WJ. ADP-ribosyl cyclase and ryanodine receptors mediate endothelin ETA and ETB receptor-induced renal vasoconstriction in vivo. *Am J Physiol Renal Physiol*. 2008;295(2):F360–F368.
29. Giulumian AD, Meszaros LG, Fuchs LC. Endothelin-1-induced contraction of mesenteric small arteries is mediated by ryanodine receptor Ca<sup>2+</sup> channels and cyclic ADP-ribose. *J Cardiovasc Pharmacol*. 2000;36(6):758–763.
30. Esporcatte BL, Tavares IM. Normal-tension glaucoma: an update. *Arq Bras Oftalmol*. 2016;79(4):270–276.
31. Schlotzer-Schrehardt U, Khor CC. Pseudoexfoliation syndrome and glaucoma: from genes to disease mechanisms. *Curr Opin Ophthalmol*. 2021;32(2):118–128.
32. European Glaucoma Society Terminology and Guidelines for Glaucoma, 5th Edition. *Br J Ophthalmol*. 2021;105(suppl 1):1–169.
33. Tribble JR, Otmani A, Sun S, et al. Nicotinamide provides neuroprotection in glaucoma by protecting against mitochondrial and metabolic dysfunction. *Redox Biol*. 2021;43:101988.
34. Tribble JR, Otmani A, Kokkali E, Lardner E, Morgan JE, Williams PA. Retinal ganglion cell degeneration in a rat magnetic bead model of ocular hypertensive glaucoma. *Transl Vis Sci Technol*. 2021;10(1):21.
35. Rutigliani C, Tribble JR, Hagstrom A, et al. Widespread retina and optic nerve neuroinflammation in enucleated eyes from glaucoma patients. *Acta Neuropathol Commun*. 2022;10(1):118.
36. Tribble JR, Hagstrom A, Jusseaume K, et al. NAD salvage pathway machinery expression in normal and glaucomatous retina and optic nerve. *Acta Neuropathol Commun*. 2023;11(1):18.

37. Nair AB, Jacob S. A simple practice guide for dose conversion between animals and human. *J Basic Clin Pharm*. 2016;7(2):27–31.
38. Rao HL, Dasari S, Riyazuddin M, et al. Referenced scans improve the repeatability of optical coherence tomography angiography measurements in normal and glaucoma eyes. *Br J Ophthalmol*. 2021;105(11):1542–1547.
39. Lim HB, Kim YW, Kim JM, Jo YJ, Kim JY. The importance of signal strength in quantitative assessment of retinal vessel density using optical coherence tomography angiography. *Sci Rep*. 2018;8(1):12897.
40. Lim HB, Kim YW, Nam KY, Ryu CK, Jo YJ, Kim JY. Signal strength as an important factor in the analysis of peripapillary microvascular density using optical coherence tomography angiography. *Sci Rep*. 2019;9(1):16299.
41. Zudaire E, Gambardella L, Kurcz C, Vermeren S. A computational tool for quantitative analysis of vascular networks. *PLoS One*. 2011;6(11):e27385.
42. Kiss T, Balasubramanian P, Valcarcel-Ares MN, et al. Nicotinamide mononucleotide (NMN) treatment attenuates oxidative stress and rescues angiogenic capacity in aged cerebrovascular endothelial cells: a potential mechanism for the prevention of vascular cognitive impairment. *GeroScience*. 2019;41(5):619–630.
43. Csizsar A, Tarantini S, Yabluchanskiy A, et al. Role of endothelial NAD<sup>+</sup> deficiency in age-related vascular dysfunction. *Am J Physiol Heart Circ Physiol*. 2019;316(6):H1253–H1266.
44. Hu X, Wang X, Dai Y, Qiu C, Shang K, Sun X. Effect of nimodipine on macular and peripapillary capillary vessel density in patients with normal-tension glaucoma using optical coherence tomography angiography. *Curr Eye Res*. 2021;46(12):1861–1866.
45. Henry E, Newby DE, Webb DJ, Hadoke PW, O'Brien CJ. Altered endothelin-1 vasoreactivity in patients with untreated normal-pressure glaucoma. *Invest Ophthalmol Vis Sci*. 2006;47(6):2528–2532.
46. Wollensak G, Schaefer HE, Ihling C. An immunohistochemical study of endothelin-1 in the human eye. *Curr Eye Res*. 1998;17(5):541–545.
47. Reinehr S, Mueller-Buehl AM, Tsai T, Joachim SC. Specific biomarkers in the aqueous humour of glaucoma patients. *Klin Monbl Augenheilkd*. 2022;239(2):169–176.
48. Li S, Zhang A, Cao W, Sun X. Elevated plasma endothelin-1 levels in normal tension glaucoma and primary open-angle glaucoma: a meta-analysis. *J Ophthalmol*. 2016;2016:2678017.
49. Resch H, Karl K, Weigert G, et al. Effect of dual endothelin receptor blockade on ocular blood flow in patients with glaucoma and healthy subjects. *Invest Ophthalmol Vis Sci*. 2009;50(1):358–363.
50. Marola OJ, Syc-Mazurek SB, Howell GR, Libby RT. Endothelin 1-induced retinal ganglion cell death is largely mediated by JUN activation. *Cell Death Dis*. 2020;11(9):811.
51. Sasaoka M, Taniguchi T, Shimazawa M, Ishida N, Shimazaki A, Hara H. Intravitreal injection of endothelin-1 caused optic nerve damage following to ocular hypoperfusion in rabbits. *Exp Eye Res*. 2006;83(3):629–637.
52. El-Nimri NW, Moghimi S, Penteado RC, et al. Comparison of the effects of latanoprostene bunod and timolol on retinal blood vessel density: a randomized clinical trial. *Am J Ophthalmol*. 2022;241:120–129.
53. Weindler H, Spitzer MS, Schultheiss M, Kromer R. OCT angiography analysis of retinal vessel density in primary open-angle glaucoma with and without Tafluprost therapy. *BMC Ophthalmol*. 2020;20(1):444.
54. Kurashima H, Watabe H, Sato N, Abe S, Ishida N, Yoshitomi T. Effects of prostaglandin F<sub>2α</sub> analogues on endothelin-1-induced impairment of rabbit ocular blood flow: comparison among tafluprost, travoprost, and latanoprost. *Exp Eye Res*. 2010;91(6):853–859.
55. Sacca SC, Rolando M, Marletta A, Macri A, Cerqueti P, Ciurlo G. Fluctuations of intraocular pressure during the day in open-angle glaucoma, normal-tension glaucoma and normal subjects. *Ophthalmologica*. 1998;212(2):115–119.
56. Nakakura S, Mori E, Fujio Y, et al. Comparison of the intraocular pressure measured using the new rebound tonometer Icare ic100 and Icare TA01i or Goldmann applanation tonometer. *J Glaucoma*. 2019;28(2):172–177.
57. Campbell P, Edgar DF, Shah R. Inter-optometrist variability of IOP measurement for modern tonometers and their agreement with Goldmann applanation tonometry. *Clin Exp Optom*. 2021;104(5):602–610.
58. Khanal S, Walton M, Davey PG. Evaluation of intraocular pressure estimates obtained using an iCare rebound tonometer. *Clin Exp Optom*. 2017;100(2):179–183.
59. Sharpe RA, Nelson LA, Stewart JA, Stewart WC. The placebo effect in early-phase glaucoma clinical trials. *Curr Eye Res*. 2015;40(6):653–656.
60. Rao HL, Pradhan ZS, Weinreb RN, et al. Determinants of peripapillary and macular vessel densities measured by optical coherence tomography angiography in normal eyes. *J Glaucoma*. 2017;26(5):491–497.
61. Nie L, Cheng D, Cen J, et al. Effects of exercise on optic nerve and macular perfusion in glaucoma and normal subjects. *J Glaucoma*. 2022;31(10):804–811.
62. Hahn SR. Patient-centered communication to assess and enhance patient adherence to glaucoma medication. *Ophthalmology*. 2009;116(11 suppl):S37–S42.